

Stochastic Orientational Relaxation of a Plastic Crystal[†]

Jun-ichi Koga* and Takashi Odagaki

Department of Physics, Kyushu University, Fukuoka 812-8581, Japan

Received: September 13, 1999; In Final Form: February 1, 2000

Dielectric properties of cyanoadamantane in the plastic phase are studied using a stochastic model for orientational relaxation. The jump rate distribution is assumed to be a power law function, and the master equation is solved within the coherent medium approximation. The orientational relaxation function is shown to be fitted well by a stretched exponential function. The exponent of the power law distribution function is related to temperature by comparing the Cole–Cole plot of the complex dielectric constant with experiments. The glass transition temperature is shown to correspond to the Vogel–Fulcher temperature where the relaxation time diverges.

1. Introduction

Orientationally disordered crystals or plastic crystals consist of nonspherical (but close-to-spherical) molecules, in which the center of mass of each molecule forms a translational order and the orientation of each molecule changes randomly. Because of this characteristic structure, plastic crystals show plasticity as their name implies. When plastic crystals are cooled, the rotational motion freezes and an orientational order appears at a certain temperature in most cases. However, under careful cooling, the rotational motion freezes keeping random orientation of molecules. This state of plastic crystals, first recognized by Suga and Seki,^{1,2} is now known as the orientational glass.

In the orientational glass forming process, plastic crystals show a dynamic and thermodynamic singularity at a certain temperature called the glass transition temperature. For example, cyanoadamantane (CNADM) exhibits the transition at $T_g = 170$ K.³ The nature of the transition has been attracting wide interests because of its relation to the structural glass transition.⁴ Although the singularities observed for the orientational glass transition are similar to those known for the structural glass transition, it is important to find out what is the correspondence between these two kinds of glass transitions.

In this paper, we study the orientational glass transition of CNADM using a stochastic model for the tumbling motion of molecules. We exploit the master equation with a random jump rate to describe the stochastic motion and calculate the frequency dependent dielectric constant. By comparing the Cole–Cole plot with experiments, we deduce the temperature dependence of a model parameter and suggest that the stochastic motion freezes at the glass transition point.

In section 2, we introduce the stochastic model for the tumbling motion and present the basic formalism to obtain the dielectric constant. We explain the coherent medium approximation which is utilized to obtain the ensemble average of the dielectric constant. Numerical results are presented in section 5 and comparison with experiments is given in section 6. We discuss the results in section 7.

2. Stochastic Model

It is known that the crystal structure of the plastic phase of CNADM is an fcc and the orientation of each molecule (direction of the dipole moment) is restricted to six cubic axes, and molecules perform tumbling motion among these six axes.^{5–7} Because of the steric hindrance between neighboring molecules, the tumbling motion of a molecule must be highly correlated to the orientation of other molecules. Despite this complex mechanism of tumbling motion, however, one can still focus on the motion of a particular molecule and consider the one-body problem of the stochastic dynamics among the six orientations.

We denote directions (0,0,1), (1,0,0), (0,1,0), (−1,0,0), (0,−1,0), and (0,0,−1) in a cubic lattice by 1, 2, 3, 4, 5, and 6, respectively, and the probability that the dipole moment is in the i th direction at time t by $p_i(t)$ when it was in direction 1 at time $t = 0$.

We employ a master equation which determines the time evolution of the probability vector $\mathbf{p}(t) = (p_1(t), p_2(t), \dots, p_6(t))$

$$\frac{d}{dt}\mathbf{p}(t) = \mathbf{p}(t)\mathbf{W} \quad (1)$$

Here, \mathbf{W} is a 6×6 matrix whose component w_{ij} ($i \neq j$) denotes the transition rate from the i th to the j th direction, and $w_{ii} = -\sum_{j \neq i} w_{ij}$ which guarantees the conservation of probability. We assume that the direct transitions from one direction to the opposite direction are not allowed, and thus the jump rate matrix takes the form

$$\mathbf{W} = \begin{bmatrix} w_{11} & w_{12} & w_{13} & w_{14} & w_{15} & 0 \\ w_{21} & w_{22} & w_{23} & 0 & w_{25} & w_{26} \\ w_{31} & w_{32} & w_{33} & w_{34} & 0 & w_{36} \\ w_{41} & 0 & w_{43} & w_{44} & w_{45} & w_{46} \\ w_{51} & w_{52} & 0 & w_{54} & w_{55} & w_{56} \\ 0 & w_{62} & w_{63} & w_{64} & w_{65} & w_{66} \end{bmatrix} \quad (2)$$

In the present one-body approach, the jump rates $\{w_{ij}\}$ are assumed to be random quantities whose distribution is determined by the many-body effects.

[†] Part of the special issue "Harvey Scher Festschrift".

* Present address: NTT Network Service Systems Laboratories.

Once the probability $p(t)$ at time t is obtained, the relaxation function of the dipole moment

$$\Phi(t) = \langle \cos\theta(t) \cos\theta(0) \rangle \quad (3)$$

can be calculated as

$$\Phi(t) = \langle p_1(t) - p_6(t) \rangle \quad (4)$$

The frequency-dependent complex dielectric constant $\epsilon(\omega) \equiv \epsilon'(\omega) - i\epsilon''(\omega)$, is defined by

$$\frac{\epsilon(\omega) - \epsilon(\infty)}{\epsilon(0) - \epsilon(\infty)} = \int_0^\infty \left\{ -\frac{d}{dt} \Phi(t) \right\} e^{-i\omega t} dt \quad (5)$$

where $\epsilon(0)$ stands for the static dielectric constant and $\epsilon(\infty)$ is the permittivity contribution due to the atomic and ionic polarizations.

Using eq 4, the dielectric constant can be obtained by

$$\frac{\epsilon(\omega) - \epsilon(\infty)}{\epsilon(0) - \epsilon(\infty)} \equiv \tilde{\epsilon}(\omega) = 1 - i\omega \langle \tilde{p}_1(i\omega) - \tilde{p}_6(i\omega) \rangle \quad (6)$$

where $\tilde{p}_i(u)$ is the Laplace transform of $p_i(t)$

$$\tilde{p}_i(u) = \int_0^\infty e^{-ut} p_i(t) dt \quad (7)$$

3. Coherent Medium Approximation

The master equation (eq 1) can be formally solved in the Laplace domain as

$$\tilde{p}(u) = p(0)(u\mathbf{1} - \mathbf{W})^{-1} \quad (8)$$

where $\mathbf{1}$ is a 6×6 unit matrix.

To obtain the dielectric constant from eq 6, we have to evaluate the ensemble average of $\tilde{p}(u)$, which can be done effectively using the coherent medium approximation (CMA).⁸

In the CMA, the ensemble averaged matrix $\langle (u\mathbf{1} - \mathbf{W})^{-1} \rangle$ is replaced by a coherent matrix $\langle (u\mathbf{1} - \mathbf{W}_C(u))^{-1} \rangle$. Here, $\mathbf{W}_C(u)$ has the same structure as eq 2 where all w_{ij} 's are replaced by a coherent jump rate $w_C(u)$ which depends on the Laplace parameter u . Because of the present form of the matrix \mathbf{W} , the condition

$$\langle (u\mathbf{1} - \mathbf{W})^{-1} \rangle = (u\mathbf{1} - \mathbf{W}_C)^{-1} \quad (9)$$

yields

$$\left\langle \frac{w_C(u) - w}{1 - 2(G_1 - G_2)(w_C(u) - w)} \right\rangle = 0 \quad (10)$$

where w is a random jump rate, and G_1 and G_2 are (1,1) and (2,1) matrix elements of $(u\mathbf{1} - \mathbf{W}_C)^{-1}$ given by

$$G_1(u) = \frac{u^2 + 6uw_C + 4w_C^2}{u(u + 4w_C)(u + 6w_C)}$$

$$G_2(u) = \frac{w_C}{u(u + 6w_C)} \quad (11)$$

Equation 10 is a nonlinear equation for $w_C(u)$ which is solved by the iteration in the following scheme

$$w_C(u) = \left\langle \frac{1}{Z + 2w} \right\rangle^{-1} - Z \quad (12)$$

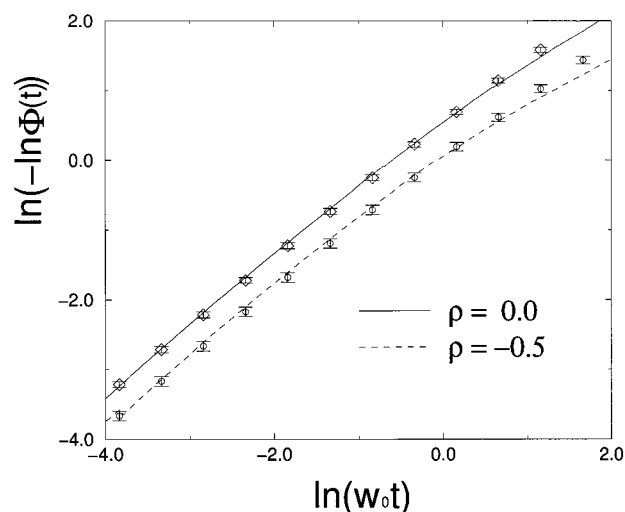


Figure 1. Rotational relaxation function for the stochastic motion defined by eq 1. Solid and dashed curves are obtained by the CMA and symbols are results of the simulation.

where

$$Z = (G_1 - G_2)^{-1} - 2w_C(u)$$

$$= \frac{u^2 + 8uw_C(u) + 14w_C^2(u)}{u + 5w_C(u)} \quad (13)$$

4. Results

We use the hopping model in which the transition rate satisfies the symmetry condition $w_{ij} = w_{ji}$. We may also use the trapping model⁹ where jump rates depend only on the origin of the jump. The results obtained by the trapping model are summarized in the Appendix. We will see that the hopping model gives better agreement with experiments.

We exploit a power law distribution function which can be derived in general for an activation process with a distributed excitation energy¹⁰ and has been successfully utilized in the theory of glass transition.¹¹ The distribution function $P(w)$ of the jump rate w is assumed to be

$$P(w) = \begin{cases} (\rho + 1) \frac{w^\rho}{w_0^{\rho+1}} & (0 \leq w \leq w_0) \\ 0 & (\text{otherwise}) \end{cases} \quad (14)$$

where ρ ($\rho > -1$) is a parameter of the model and w_0 determines the scale of time of the model. We solved eqs 12 and 14 by iteration and determined the coherent jump rate as a function of frequency, which in turn was utilized to obtain the relaxation function from eq 4 and the dielectric function from eq 6.

To test the accuracy of the CMA, we first obtained the time dependence of the relaxation function $\Phi(t)$ and compared it to the result obtained by a Monte Carlo simulation of the stochastic motion of a molecule. Figure 1 shows the comparison in which $\ln[-\ln \Phi(t)]$ is plotted against $\ln t$. Agreement of both results is satisfactory in this time window. Figure 1 also indicates that the relaxation function can be fitted well by the stretched exponential function $\exp[-(t/\tau)^\beta]$ with $\beta \sim 0.8$.

Figures 2 and 3 show the real and imaginary part of $\tilde{\epsilon}(\omega)$, respectively. As one can see in Figures 2 and 3, the dielectric constant is close to the Debye relaxation for large ρ , but it deviates from the Debye behavior significantly when $\rho < 0$.

We define the relaxation time by the inverse of the frequency at which the imaginary part of the dielectric constant takes a

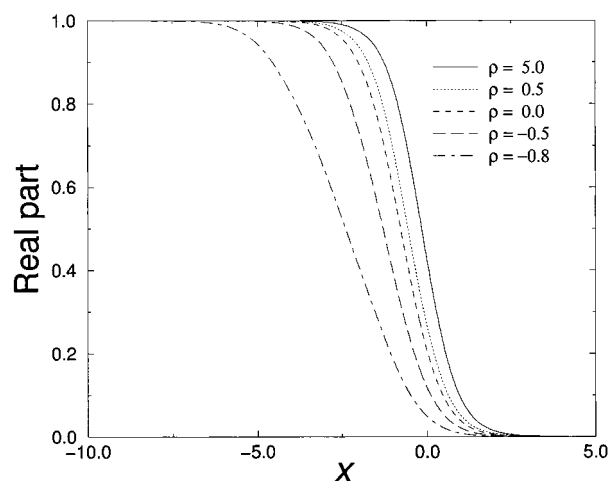


Figure 2. Frequency dependence of the real part of $\tilde{\epsilon}(\omega)$. $x = \ln(\omega/4\omega_0)$.

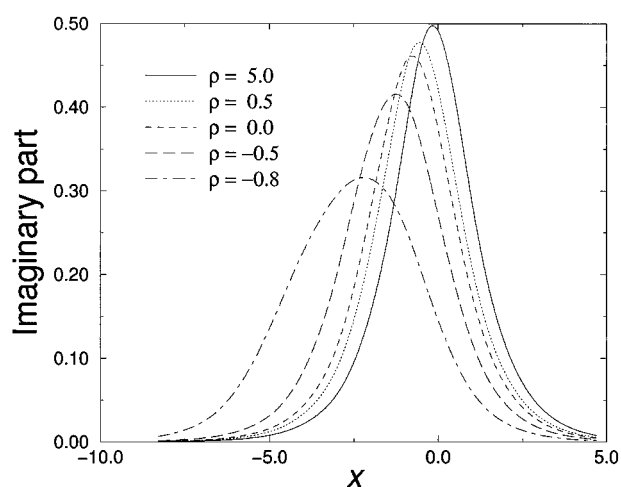


Figure 3. Frequency dependence of the imaginary part of $\tilde{\epsilon}(\omega)$. $x = \ln(\omega/4\omega_0)$.

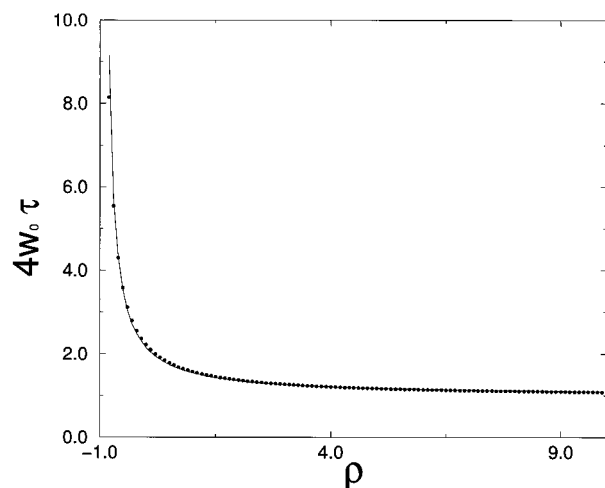


Figure 4. The relaxation time is plotted against ρ . The solid curve is the fit by eq 15.

maximum. Figure 4 shows the dependence of the relaxation time on parameter ρ . The relaxation time can be fitted by

$$\tau = \frac{0.244}{\omega_0} \left(\frac{\rho + 2}{\rho + 1} \right)^{1.18} \quad (15)$$

which diverges at $\rho = -1$. Thus $\rho = -1$ can be considered to

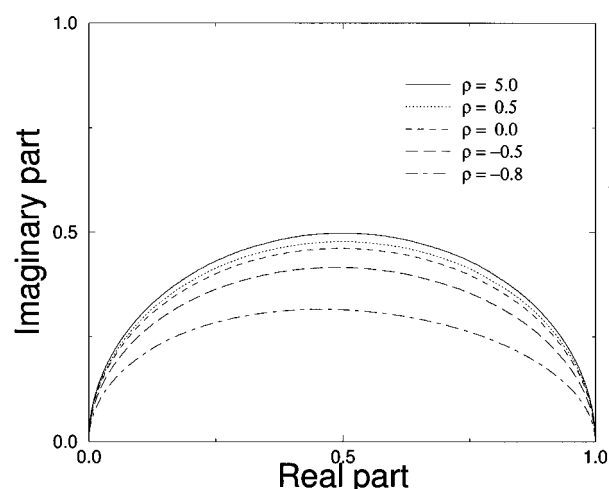


Figure 5. Cole–Cole plot of the dielectric constant of the stochastic model. The imaginary part of $\tilde{\epsilon}(\omega)$ is plotted against the real part of $\tilde{\epsilon}(\omega)$.

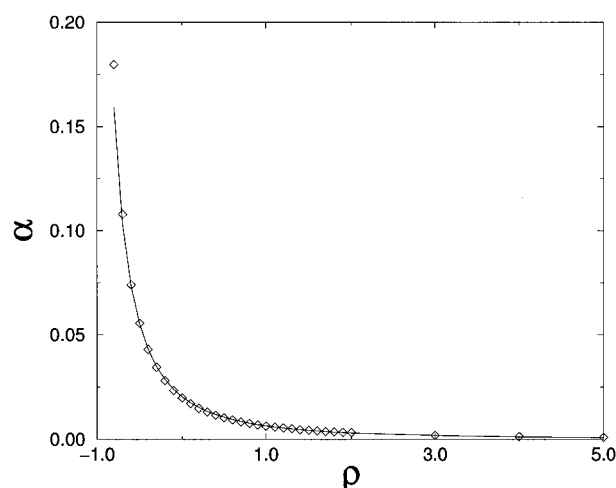


Figure 6. Relation between ρ and α . The solid curve is a guide for the eye.

correspond to the Vogel–Fulcher temperature of the structural glass forming materials.¹²

The characteristics of the dielectric constant $\tilde{\epsilon}(\omega)$ are usually analyzed by the Cole–Cole plot in which the imaginary part of $\tilde{\epsilon}(\omega)$ is plotted against the real part of $\tilde{\epsilon}(\omega)$. Figure 5 shows the Cole–Cole plot for various values of parameter ρ .

When ρ is large, the Cole–Cole plot is close to the Debye semicircle, and it deviates from the semicircle when ρ is small, in particular for $\rho < 0$. We can fit the Cole–Cole plot by that for the Cole–Cole form of the dielectric constant

$$\epsilon(\omega) = \epsilon(\infty) + \frac{\epsilon(0) - \epsilon(\infty)}{1 + (i\omega\tau)^{1-\alpha}} \quad (16)$$

except for very small and very large frequencies. Figure 6 shows parameter α determined for various values of ρ by adjusting the maximum of the Cole–Cole plot.

The Debye relaxation corresponds to $\alpha = 0$, and thus the deviation from the Debye relaxation becomes significant for $\rho < 0$.

5. Comparison with Experiments

Experimental data for the dielectric constant of CNADM can be fitted by the Cole–Cole function, and parameter α has been

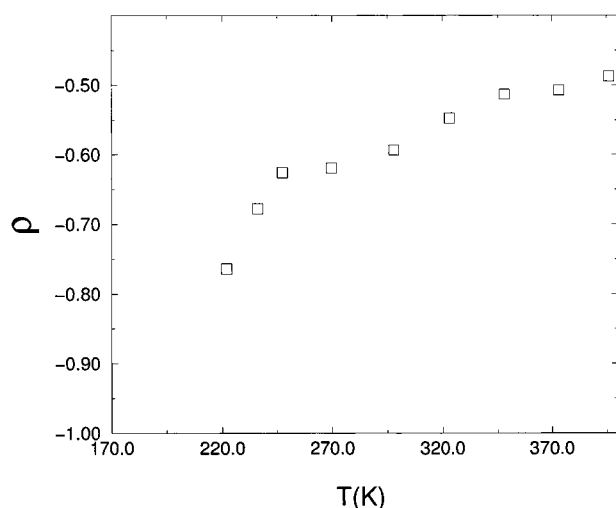


Figure 7. Temperature dependence of parameter ρ for CNADM.

determined for various temperatures.¹³ Therefore, using Figure 6, we can determine the value of parameter ρ at each temperature as shown in Figure 7.

The number of data points are not enough to determine ρ near the glass transition point. Nevertheless it is tempting to note that a smooth extrapolation of the relation between T and ρ toward the glass transition point yields $\rho \sim -1$ at $T_g = 170$ K. If the extrapolation is correct, this suggests that the orientational glass transition point is related to the divergence of the relaxation time corresponding to the Vogel–Fulcher point of the structural glass forming materials. However, it should be remarked that the relaxation around 220 K may not be fitted by the Cole–Cole function but by the Cole–Davidson function.¹⁴ If this is the case, parameter ρ may approach -1 at temperature lower than T_g .

6. Discussion

We have presented a stochastic model for the orientational motion of CNADM in the plastic phase. Exploiting the hopping model and a power law function for the jump rate distribution, we obtained the dielectric constant within the coherent medium approximation. Although the proposed model is based on one-body dynamics, it reproduces characteristic features of the Cole–Cole plot observed for CNADM. In particular, we were able to determine the temperature dependence of the model parameter and obtain results which suggest that the orientational glass transition point may correspond to the Vogel–Fulcher point of structural glass formers. At present, we do not have a clear reasoning for the relation between the power law distribution and the correlated dynamics of molecules, and therefore it is an important problem to find such a reasoning.

It should be mentioned that the Cole–Cole plot of the present model does not coincide with that of the Cole–Cole function in the limits of $\omega \rightarrow 0$ and $\omega \rightarrow \infty$; the former has an infinite slope in the limits, but the latter has a finite slope. Thus it is interesting to test the slopes of the Cole–Cole plot of CNADM in these limits. It should also be remarked that the extrapolation in Figure 7 strongly depends on the quality of experimental data and thus more reliable analysis for relaxation data is needed to obtain conclusive results.

The present model is based on the hopping model for the stochastic dynamics. For the structural glass transition, it is believed that the trapping model for the stochastic model is appropriate.¹¹ As we show in the Appendix, the Cole–Cole plot

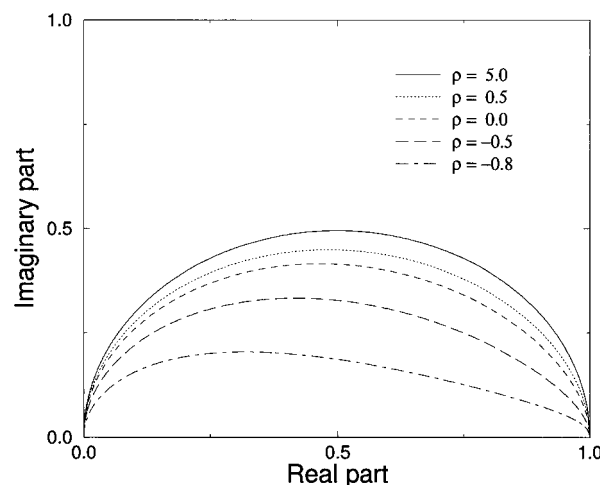


Figure 8. Cole–Cole plot of $\tilde{\epsilon}(\omega)$ for the trapping model.

of the dielectric constant for the trapping model is asymmetric and does not seem to be compatible with experiments.

Acknowledgment. It is a great honor for T. O. to dedicate this article to Hervey Scher on the occasion of his 60th birthday. This work was supported in part by Grant-in-Aid for Scientific Research (C) from the Ministry of Education, Science, Sports and Culture.

Appendix Trapping Model

For the trapping model,⁹ the jump rate w_{ij} ($i \neq j$) in eq 2 is assumed to be independent of j .¹¹ The coherent medium approximation can be obtained in the same way which reads as

$$\left\langle \frac{1}{Z + w} \right\rangle = \frac{1}{Z + w_c(u)} \quad (17)$$

where

$$Z = \frac{u^2 + 6uw_c(u) + 4w_c^2(u)}{4(u + 5w_c(u))} \quad (18)$$

The Cole–Cole plot of the dielectric constant for the trapping model is shown in Figure 8.

References and Notes

- (1) Adachi, K.; Suga, H.; Seki, S. *Bull. Chem. Soc. Jpn.* **1968**, *41*, 1073.
- (2) Suga, H.; Seki, S. *J. Non-Cryst. Solids* **1974**, *16*, 171.
- (3) Ishikawa, M.; Yamamuro, O.; Matsuo, T.; Takakura, H.; Achiwa, N. *J. Korean Phys. Soc.* **1998**, *32*, S842.
- (4) Benkof, S.; Kudlik, A.; Blochowicz, T.; Bössler, E. *J. Phys.: Condens. Matter* **1998**, *10*, 8155.
- (5) Amoureux, J. P.; Noyel, G.; Foulon, M.; Bee, M.; Jorat, L. *Mol. Phys.* **1984**, *52*, 161.
- (6) Descamp, M.; Caucheteux, C.; Odou, G.; Sauvajol, J. L. *J. Phys. Lett. (Paris)* **1984**, *45*, L719.
- (7) Kuchta, B.; Descamps, M.; Affouard, F. *J. Chem. Phys.* **1998**, *109*, 6753.
- (8) Odagaki, T.; Lax, M. *Phys. Rev. B* **1981**, *24*, 5284.
- (9) Odagaki, T. *J. Phys. A* **1987**, *20*, 6455.
- (10) Odagaki, T. *Phys. Rev. Lett.* **1995**, *75*, 3701.
- (11) Odagaki, T.; Hiwatari, Y. *Phys. Rev. A* **1990**, *41*, 929. Odagaki, T.; Matsui, J.; Hiwatari, Y. *Phys. Rev. E* **1994**, *49*, 3150.
- (12) Vogel, H. *Phys. Zeit.* **1921**, *22*, 645. Fulcher, G. S. *J. Am. Ceram. Soc.* **1925**, *8*, 339.
- (13) Amoureux, J. P.; Catelai, M.; Benadda, M. D.; Bee, M.; Sauvajol, J. L. *J. Phys. (Paris)* **1983**, *44*, 513.
- (14) Pathmanathan, K.; Johari, G. P. *J. Phys.: Condens. Matter* **1985**, *18*, 6535.